STUDY OF TOTAL ELECTRON CONTENT AND ELECTRON DENSITY PROFILE FROM SATELLITE OBSERVATIONS DURING GEOMAGNETIC STORMS

B. B. Rana, N. P. Chapagain, B. Adhikari, D. Pandit, K. Pudasainee, Shaswat Chapagain, D. Chhatkuli

Journal of Nepal Physical Society

Volume 5, Issue 1, October 2019

ISSN: 2392-473X

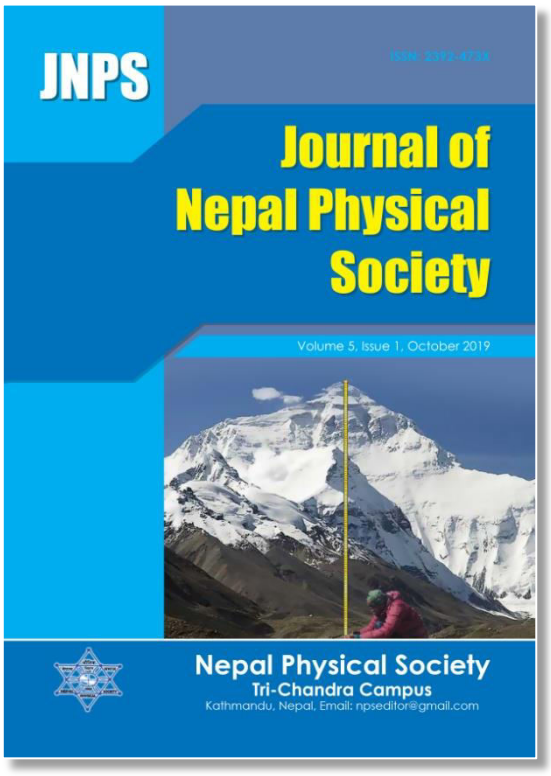

JNPS, **5** (1), 59-66 (2019)

Published by:

Nepal Physical Society

P.O. Box: 2934

Tri-Chandra Campus

Kathmandu, Nepal

Email: npseditor@gmail.com

JNPS 5 (1), 59-66 (2019)
ISSN: 2392-473X

Research Article

STUDY OF TOTAL ELECTRON CONTENT AND ELECTRON DENSITY PROFILE FROM SATELLITE OBSERVATIONS DURING GEOMAGNETIC STORMS

B. B. Rana[1], N. P. Chapagain[1], B. Adhikari[1, 2], D. Pandit[2, 3*], K. Pudasainee[2], S. Chapagain[4], D. Chhatkuli[5]

[1]*Patan Multiple Campus, Patandhoka, Lalitpur, Nepal*
[2]*St. Xavier's College, Maitighar, Kathmandu, Nepal*
[3]*Central Department of Physics, Tribhuvan University, Kirtipur, Kathmandu, Nepal*
[4]*The University of Utah, Salt Lake City, UT 84112, USA*
[5]*Tri-Chandra Multiple Campus, Ghantagar, Kathmandu*
***Corresponding Email:** pandit_drab@yahoo.com*

ABSTRACT

Total Electron Content (TEC) and electron density profile are the key parameters in the mitigation of ionospheric effects on radio wave communication system. In this study, the variations of TEC and electron density profile have been analyzed using satellite data from four different latitude-longitude sectors (13˚N - 17˚N, 88˚E - 98˚E), (30˚N - 50˚N, 95˚W - 120˚W), (26˚S - 29˚S, 163˚W - 167˚W,) and (45˚S - 60˚S, 105˚W -120˚W) during different geomagnetic storms. The interplanetary magnetic field (Bz), solar wind velocity (Vsw), solar wind pressure (Psw) and geomagnetic indices, aurora index -AE, Kp and disturbed stormed time index (Dst) are also analyzed to distinguish their effects on TEC and electron density. The geomagnetic indices and solar wind parameters are correlated with the TEC and electron density. The study showed that the value of TEC and electron density vary significantly with different latitude, longitude, altitude and solar activities. The result also concludes that the electron density profile increases with the altitude, acquired peak value around 250km-300km and decreased beyond the altitude of 300 km.

Keywords: Electron density, Geomagnetic storm, Solar wind parameters, Total electron content (TEC)

INTRODUCTION

The Earth's atmosphere has both spatial and temporal changing environment due to ionization effect of high-energetic solar radiation of extreme ultraviolet (EUV) and X-ray and it is also affected by solar wind and its geomagnetic activity [1]. A number of linearly and nonlinearly variable phenomena have been observed in ionosphere which effect the radio wave communication and navigation signal in their group delay, phase advance in carrier wave, Faraday polarization, refraction, Doppler shift, scintillation etc [1, 2]. The temporal and spatial variations include periodic variations such as daily, monthly, seasonal, annual variation and the momentary disturbance [3, 4]. The regional characteristics of low latitude ionosphere is influenced by three important electrodynamical features such as equatorial electrojet (EEJ), counter electrojet (CEJ) and equatorial ionization anomaly (EIA) [5-10]. Solar flare, geomagnetic storm, earthquake etc. are the sources of momentarily disturbance in ionosphere. Liu *et al.* [8] found the global effect of solar activities on ionosphere is high during day time than night, it effects more at low latitude than at high and maximum effect was seen on either side of the dip equator than around lower side of dip equator[8]. Meng *et al.* [11] found that the TEC outside the aurora was higher than inside the aurora and also reported that its value was more outside aurora than at the polar cap. The long term ionospheric TEC variation for the period of 1975-1980 and 1980- 1989 over Delhi in India has been studied by Gupta and Singh [12]. The variation in TEC at different regions of equatorial anomaly region are studied by several researchers [12-14]. The TEC variation in low and middle latitude of ionosphere along with the altitude using GPS satellite system has been studied by Komjathy and Shim [15, 16].

Besides ionization to the atom or molecules due to solar and cosmic radiation, the recombination between cations and free electrons takes to form neutral atoms and molecules and also the free electron gets attached to the neural molecules to form negative ion. Only the free electron effects the radiation passing through it but not the cation and anions due to large mass and inability to oscillate [17]. The impact of solar indices i.e. Solar Extreme Ultraviolet (EUV), $F_{10.7}$ solar flux and smooth sunspot number (SSN) on TEC in different seasons are studied by Chauhan [18] and Dabas [19]. Their study showed that TEC has nonlinear variation with SSN and linear variation with EUV and $F_{10.7}$ solar flux. The chemical presents in D-region are quite complex which involve O, O_2, O_3, NO, NO_2, CO_2, H_2O and alkali metals. The ionization in this region occurs due to X-rays, cosmic rays and Lyman series-alpha hydrogen of wavelength 121.5 nm. The D region is only present during daylight (the time during the sun is illuminating the ionosphere, which is considerably longer than terrestrial daylight). This region may affect the lower frequencies transmitted wave such as MW and may be coupled hundred km during daytime. The main ions composition found in the E and F-region are NO^+, O_2^+, O^+ and N_2^+ which are ionized by soft X-rays and extreme ultra-violet rays (EUV). At night time E and sporadic E (thin patches of extra ionization) are produced due to electron and meteor bombardment.

Some sporadic E radio reflections may be due to turbulence in E layer [20, 21]. In the upper F-region ionized molecules are mainly O^+, H^+ and He^+. At night due to slow recombination process between ions and electrons this layer can reflect radio signals. The ionospheric plasma density is not constant; it varies with change in altitude, latitude, longitude, season, solar and geomagnetic activity. During geomagnetic storm charged particles injected deeper into the inner magnetosphere and its effect can be predominantly strong when increased solar wind pressure is associated with an enormous southward IMF component [22]. This phase is finally followed by the recovery phase (which can last for many days) and characterized by the occurrence of several possible powerful substorms [23].

In this paper, we analyzed the variation of TEC and electron density profile of ionosphere with the different latitude, longitude and altitude during different geomagnetic storms using GRACE satellite data. For this, we have selected four different events in the same year of 2008 including one geomagnetic quiet time. These events are divided on the basis of Kp and north south interplanetary magnetic field (Bz) value. At last a collective comparison of the electron density profile for all the events has been analyzed.

DATA AND METHODS

For this research, we used internet base data provided by the international space research center – Operating Mission as Nodes on the Internet (OMNI) web system and Gravity Recovery and Climate Experiment (GRACE) satellite system. OMNI web system data is used to identify four different types of events and its respective TEC and electron density profile data taken from GRACE satellite system. These data are provided by COSMIC Data Analysis and Archive Centre (CDAAC) of the University Corporation for Atmospheric Research (UCAR). The high-resolution data for OMNI and UCAR is downloaded from web site at http://omniweb.gsfc.nasa.gov/ow_min.html and www.cosmic.ucar.edu/. The date and time of the data used in our research are tabulated in following Table 1.

Table 1: Selected events with date and time.

Events	Date	Time
Event-1	6 April 2008	0917
Event-2	27 March 2008	2221
Event-3	4 September 2008	0306
Event-4	11 October 2008	0759

RESULTS AND DISCUSSIONS

According to Gonzalez *et al.* [24], geomagnetic storms be classified on the basis of Dst as: weak ($-50 < Dst \leq -30$nT), moderate ($-100 < Dst \leq -50$nT), intense ($-250 < Dst \leq -100$nT), and very intense ($Dst \leq -250$nT). The event-1 has the minimum Dst value -35 nT so it is weak storm event whereas the minimum Dst value of event 2, 3 and 4 are -60 nT, -55 nT and -77nT respectively implies they are moderate events. Dst has acquired minimum value only for short interval of time, which is indicted by the arrow in the AE panel. Our main objective is to study the variation of TEC and electron density with longitude and latitude and also electron density with altitude at those points during these storms.

Observed Geomagnetic Indices and Solar Wind Parameters

Figure-1 represents variation in interplanetary magnetic field (Bz), plasma velocity (Vsw), plasma pressure (nPa), Kp, Dst and AE on OMNI datasets during the Event-1, 05-07 April 2008. The first row of this panel shows that Bz value has decreased to the minimum value -4 nT the second and third row of this panel show plasma velocity and pressure has consistent value. The fourth row indicates the value of Kp has not exceed 5 and fifth row shows Dst acquire a minimum value -35 nT. Similarly, the AE index ranges from 0 to peak value of 1000 nT and the Dst value approaches -35 nT for only short interval of time which is indicated by double arrow in the AE panel. The observed values of Bz, Dst and plasma speed during this event indicates it is a weak geomagnetic storm.

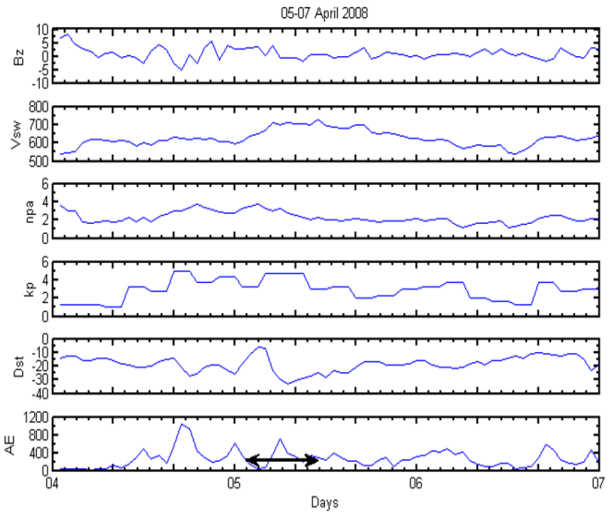

Fig.1: *From top to bottom, the panels show the variations of the south-north component of interplanetary magnetic field Bz (nT) in GSM coordinate system, solar wind plasma speed Vsw, (km/s), pressure flow(nPa), Kp, Dst (nT) and AE (nT) indices with time (days) respectively. The double arrow in the AE panel marks the minimum value in Dst for event-1, 5-7 April 2008, 0917 UT.*

Figure-2 shows the variation in interplanetary magnetic field (Bz), plasma velocity (Vsw), plasma pressure (nPa), Kp, Dst and AE on OMNI datasets during the Event-2, 26-28 march 2008. The first row of this panel shows that Bz value has decreased to -6 nT, the second and third row of this panel show plasma velocity and pressure has consistent value. The fifth row indicates the value of Kp lies between 0 to 5 and sixth row show Dst acquire a minimum value -60 nT during this event. Similarly, it shows the AE index ranges from 0 to peak value of 800 nT. In this event, the Dst value approaches -60 nT for only short interval of time which is indicated by double arrow in the AE panel. The observed values of Bz, Dst and plasma speed during this event indicates it as moderate geomagnetic storm.

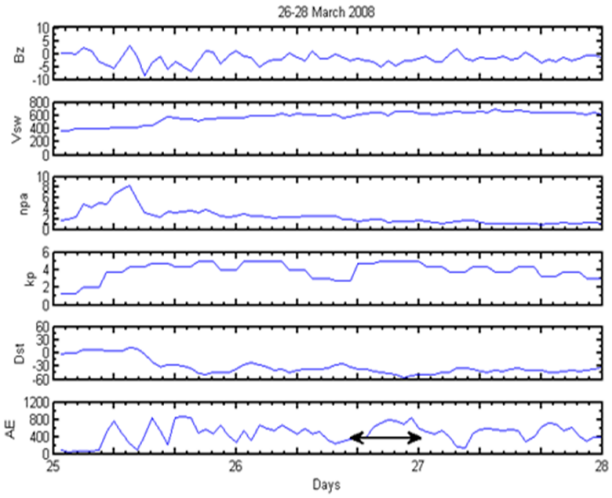

Fig. 2: *From top to bottom, the panels show the variations of the interplanetary component of magnetic field Bz (nT) in GSM coordinate system, solar wind plasma speed Vsw (km/s), flow pressure(nPa), Kp, Dst (nT) and AE (nT) indices with time (days) respectively. The double arrow in the AE panel marks the minimum value of Dst for event-2, 26-28 March 2008, 2221UT.*

Figure-3 represents variation in interplanetary north-south component of magnetic field (Bz), plasma velocity (Vsw), plasma pressure (nPa), Kp, Dst and AE on OMNI datasets during the Event-3, 03-05 September 2008. The first row of this panel shows that the interplanetary magnetic field Bz value has decreased to -12nT, the second indicates consistent value in plasma velocity whereas the third row indicates variation in plasma pressure from 1npa to 6 npa. The fifth row indicates the value of Kp has not exceed 6 and sixth row show Dst acquire a minimum value -55 nT. Similarly, it shows the AE index ranges from 0 to peak value of 1250 nT. In this event, the Dst value approaches -55 nT for only short interval of time which is indicated by double arrow in the AE panel. The observed values of Bz, Dst and plasma speed during this event indicates it as moderate geomagnetic storm.

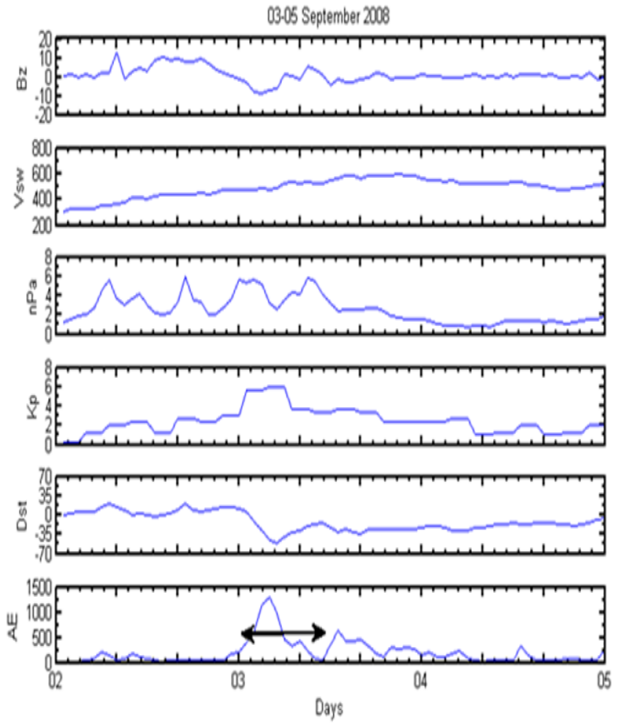

Fig. 3: *From top to bottom, the panels show the variations of the south-north component of magnetic field Bz(nT) in GSM coordinate system, solar wind plasma speed, Vsw, (km/s), pressure flow(nPa), Kp, Dst (nT) and AE (nT) indices with time (days) respectively. The double arrow in the AE panel marks the minimum value of Dst for event-3, 03-05 September 2008, 0306 UT.*

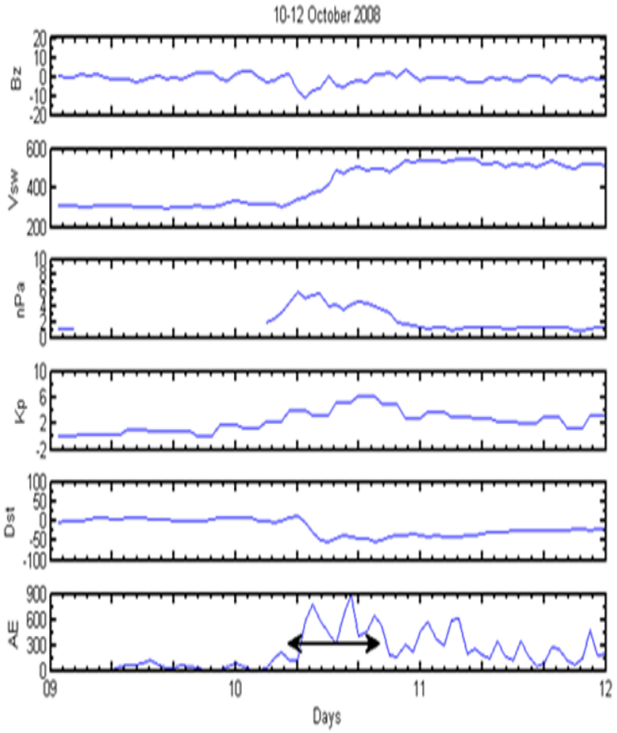

Fig. 4: *From top to bottom, the panels show the variations of the south-north component of magnetic field Bz (nT) in GSM coordinate system, solar wind plasma speed, Vsw, (km/s), pressure flow(nPa), Kp, Dst (nT) and AE (nT) indices with time (days) respectively. The double arrow in the AE panel marks the minimum value of Dst for event-4, 10-12 October 2008, 0759 UT.*

Figure-4 shows variation in interplanetary north-south magnetic field (Bz), plasma velocity (Vsw), plasma pressure (nPa), Kp, Dst and AE on OMNI datasets during the Event-4, 10-12 October 2008. The first row of this panel shows that the interplanetary magnetic field Bz value has decreased to -16nT, the second panel indicates value of plasma velocity has consistent value before the event day but increases its value 575Km/s and then it becomes consistent in plasma velocity whereas the third row indicates variation in plasma pressure from 2npa to 6 npa. The fifth row indicates the value of Kp has value between 0 to 6 and sixth row show Dst acquire a minimum value -77 nT during this event. Similarly, the last row shows the AE index ranges from 0 to peak value of 900 nT. In this event, the Dst value approaches -77 nT for only short interval of time which is indicated by double arrow in the AE panel. The observed values of Bz, Dst and plasma speed during this event indicates it as moderate geomagnetic storm.

Observed TEC and Electron Density Variations

Among four selected events, event-1 describes for quiet day and the other 3 events are for moderate storm days. In this section we have analyzed the effect of storm on TEC and electron density and also the variation in TEC and electron density profile with latitude, longitude and altitude. Finally, their comparative study is summarized in table -2.

In figure 5, plots (A) and (C) show the variation of total electron content and electron density with latitude from 13˚N to 17˚N. It observed that both TEC and electron density increase with latitude and acquired the maximum value 350 TECU and $12.5x10^5$ el/cm^3, respectively near 15˚N latitude and then decreases. The plots (B) and (D) in figure5 show variation of TEC and electron density with longitude from 88˚E to 98˚E. It shows that TEC and electron density increases with longitude and acquires the maximum value 350 TECU and $12.5x10^5$ el/cm^3, respectively at longitude 94˚E and then decreases.

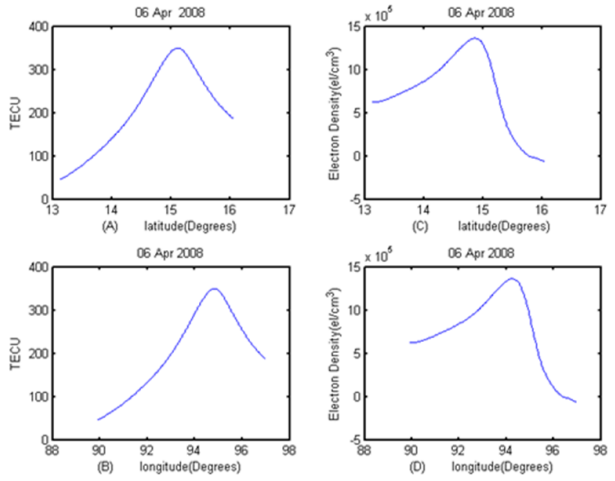

Fig. 5: *The variations of (A) TEC (TECU) with latitude (degree), (C) electron density (el/em3) with latitude (degree), (B) TEC (TECU) with longitude (degree) and (D) electron density (el/em3) with longitude (degree) for event-1, 6th April 2008, 0917 UT.*

Similarly, in figure 6, plots (A) and (C) show the variation of total electron content and electron density with latitude from 30˚N to 50˚N. It is observed that both TEC and electron density increase with latitude and acquired the maximum value of 170 TECU and $6x10^5$ el/cm^3 respectively near 44˚N latitude and then decreases. The plots (B) and (D) in figure 6 show variation of TEC and electron density with longitude from 120˚W to 95˚W.

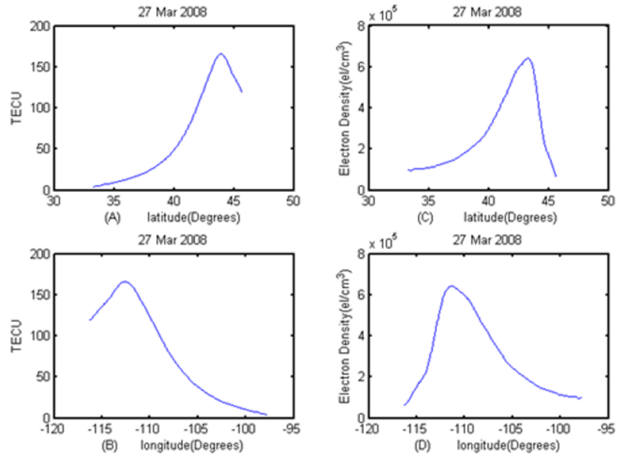

Fig. 6: *The variations of (A) TEC (TECU) with latitude (degree), (C) electron density (el/em3) with latitude (degree), (B) TEC (TECU) with longitude (degree) and (D) electron density (el/em3) with longitude (degree) for event-2, 27th March 2008, 2221UT.*

Figure 7 also plots the variation of TEC and electron density with latitude from 29˚S to 26˚S. It is observed that TEC and electron density has maximum value of 94 TECU and $3.75x10^5$ el/cm^3 respectively near 28.5˚S latitude. In plots (B) and (D), TEC and electron density have the maximum values 94 TECU and $3.5x10^5$ el/cm^3, respectively at the longitude 164.5˚W.

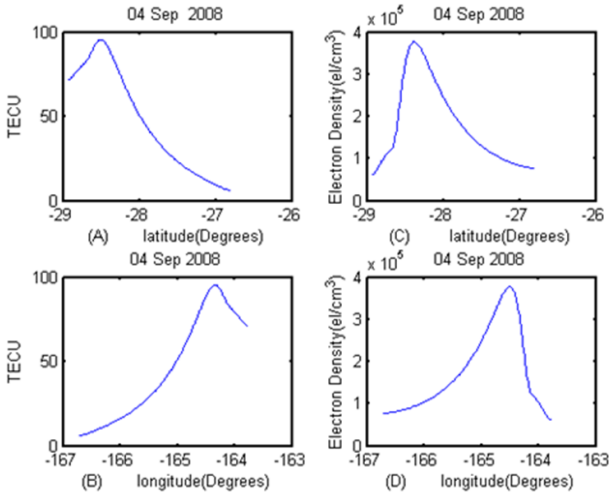

Fig. 7: *The variations of (A) TEC (TECU) with latitude (degree), (C) electron density (el/cm3) with latitude (degree), (B) TEC (TECU) with longitude (degree) and (D) electron density (el/cm3) with longitude (degree) for event-3, 4th September 2008, 0306 UT.*

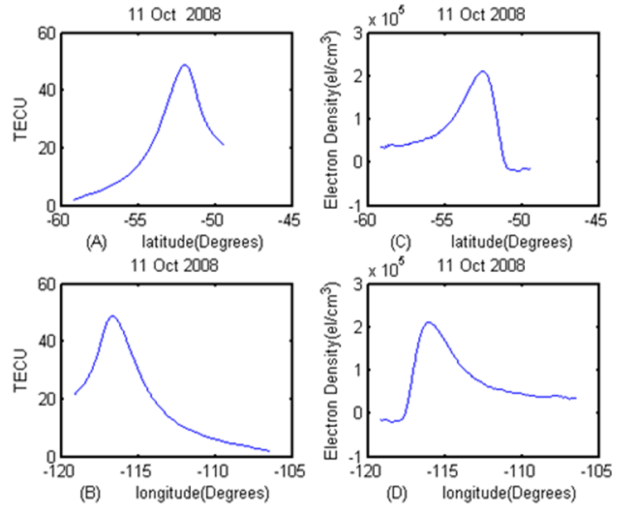

Fig. 8: *The variations of (A) TEC (TECU) with latitude (degree), (C) electron density (el/em3) with latitude (degree), (B) TEC (TECU) with longitude (degree) and (D) electron density (el/cem3) with longitude (degree) for event-4, 11th October 2008, 0759 UT.*

Similarly, in figure 8, plots (A) and (C) show the variation of total electron content and electron density with latitude acquiring the maximum value of 50 TECU and $2.5x10^5$ el/cm^3 respectively near 52˚S latitude. The plots (B) and (D) in figure 8

show variation of TEC and electron density with longitude showing the maximum values of 50 TECU and $2.5x10^5$el/cm^3, respectively at the longitude 116˚W and then decreases.

Table 2: Summary of the maximum values of Bz, Kp, electron density and TEC for event 1 to 4 obtained from figure 1 to 8 respectively.

Events	Date/Time (UT)	Geo position	Bz (nT)	Kp	Electron Density (el/cm^3)	TEC (TECU)
1.	6th April 2008, 0917	Lat(13˚N to17˚N) Lon(88˚E to 98˚E)	-4	5	$12.5x10^5$	350
2.	27th March 2008, 2221	Lat(30˚N to 50˚N) Lon(120˚W to 95˚W)	-6	5	$6x10^5$	170
3.	4th September 2008, 0306	Lat(29˚S to 26˚S) Lon(167˚W to 163˚W)	-12	6	$3.75x10^5$	94
4.	11th October 2008, 0759	Lat(60˚S to 45˚S) Lon(120˚W to 105˚W)	-16	6	$2.5x10^5$	50

The variation in TEC and electron density varies with day of the time, latitude-longitude, seasonal and activity of the Sun. Photoionization of neutral atoms or molecules due to X-rays and EUV radiation and collision with precipitated particle during geomagnetic storm time varies the number of plasma in the ionosphere. Under influence of geomagnetic field these plasmas are transported through neutral wind and electric field by gravitational and plasma pressure gradient forces [23]. In 1995 Su *et al.* [25] found that longitudinal difference in TEC during day time by the difference in neutral wind velocity whereas during night time it is due to the difference in neutral wind velocity and the $\vec{E}X\vec{B}$ drift velocities. The TEC and electron density value are found to be decreased from event-1 to event-4 as the strength of negative geomagnetic storm become stronger which is similar with the results obtained in different papers [26-29].

Electron Density Variations with Altitude

In figure 9, the electron density increases with altitude and acquired a maximum value at particular attitude then decreases. The green, blue, black and red color curves represent event-1 to event-4 respectively. In event-1, it is observed that the electron density acquired maximum value $13x10^5$el/cm^3 around 300 km. Blue curve shows maximum value of electron density is $6.5x10^5$el/cm^3 during event-2 near the altitude 250 km. Black curve shows the peak value of electron density during event-3 is $3.75x10^5$ el/cm^3 near 250 km. Similarly, red color reflects the electron density profile of event-4 which has a peak value $2x10^5$ el/cm^3 around 300 km. The graph showed the magnitude of peak electron density decreased with the increase in strength of the geomagnetic storm. The results also indicate that the peak electron density lies in the altitude ranges of 250-300 km.

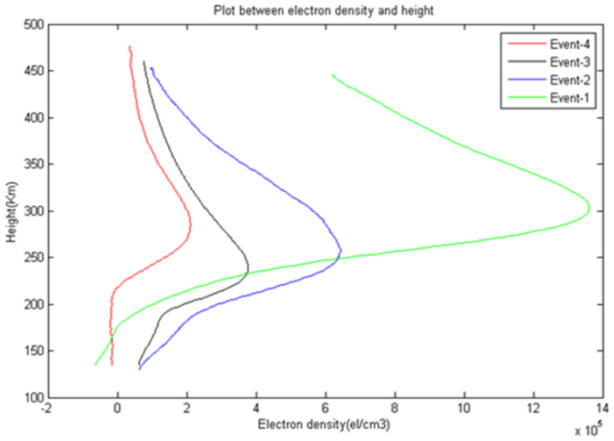

Fig. 9: *Shows profile of electron density (el/cm3) with altitude (km) for event 1 to 4.*

This result is good agreement with the result found in papers [26-29]. The latitude, local time and phase of storm play the important role in the occurrence of positive and negative storm [30]. These primary driving mechanisms responsible for different storms are widely investigated and documented in the papers by Mendillo [31]; Buonsanto [32]. In Mendillo [31] paper it was described that in summer hemisphere negative phase storm occurs with greater probability and positive storm is prominent in winter hemisphere.

It is accepted that negative storm is generated by change in neutral composition and positive storm by composition changes [4, 31-34]. In 1993 Prolss gave an idea for time sequence thermospheric-ionospheric storm based on the fact that positive storms are attributed to meridional wind and change in neutral composition caused negative ionospheric wind. During geomagnetic storms, the energy input from the magnetosphere to the atmosphere is increased, which enhances the joule heating at high latitudes. This decreases the normal poleward wind on the dayside and strengthens the equator-ward wind on the night side, thereby creating a storm circulation which creates increase in molecular species to the mid-latitudes. The movement of the neutral composition and increase in loss rate can significantly reduce the F-region electron density to the mid latitude which may be the cause to decrease in electron density during increase in strength of geomagnetic storm [33].

CONCLUSIONS

We have studied the variations of TEC and electron density with latitude and longitude as well as variations of electron density with altitude during four different geomagnetic storms which are classified on the basis of geomagnetic indices and solar wind parameters such as Kp, Dst, AE index and interplanetary magnetic field (Bz), plasma drift speed (Vsw) and flow pressure (nPa), respectively. The events were quiet to moderate lying at four different locations- (latitude, longitude): (13˚N -17˚N, 88˚E - 98˚E), (30˚N-50˚N, 120˚W -95˚W), (29˚S-26˚S, 167˚W-163˚W) and (60˚S-45˚S, 120˚W-105˚W). The analysis showed the significant variations of TEC and electron density with latitude, longitude, respectively. All the results are similar irrespective to the geomagnetic conditions. For event 1 to 4 the peak value of electron densities and TEC are found to be $12.5x10^5$ el/cm^3, $6x10^5$ el/cm^3, $3.75x10^5$ el/cm^3, $2x10^5$ el/cm^3; 350, 170, 94, 50 TECU, respectively. The value of TEC and electron density found to be decreased from event-1 to event-4 with increase in negative value of Bz. Likewise, the similar nature of the curve is obtained for the variations in electron density profile with altitude for event 1 to 4 but the magnitude of electron density was found to be decreasing as the strength of geomagnetic storm increased.

ACKNOWLEDGEMENTS

This work was supported by Department of Physics, Patan Multiple Campus. B. B. Rana gave special thanks to the office of B. P. Koirala Memorial Planetorium, Observatory and Science Museum Development Board (BPKMPOASMDB), Kirtipur Kathmandu for providing scholarships to to carry out this research projects and complete master dissertation. The data sets for this study were downloaded from NASA website (http://omniweb.gsfc.nasa.gov/ow_min.html. and www.cosmic.ucar.edu/). We would like to thank staff members from NASA.

REFERENCES

[1] Guo, J; Li, W.; Liu, X.; Kong, Q; Zhao, C. and Guo, B. Temporal-Spatial Variation of Global GPS Derived Total Electron Content, *PLOSONE*, **10**, 1999–2013. e0133378. doi:10.1371/journal. pone.01333782 (2015).

[2] Hajra, R.; Chakraborty, S.K.; Tsurutani, B.T.; Gupta, A.D. ; Echer, E; Brum, C.G.M., Gonzalez, W.D and Sobral, J.H. An empirical model of ionospheric total electron content (TEC) near the crest of the equatorial ionization anomaly (EIA), *.J. Space Weather Space Clim.,***A29**.6 (2016)**.**

[3] Xu, J.S.; Li, X.J.; Liu, Y.W. and Jing, M. Effects of declination and thermospheric wind on TEC longitude variations in the mid-latitude ionosphere. *Chinese Journal of Geophysics.***56**: 1425–1434 (2003). doi: 10.6038/cjg20130501.

[4] Adhikari, B.; Khatiwada, R. and Chapagain, N. P. Analysis of Geomagnetic Storms Using Wavelet Transforms, *Journal of Nepal Physical Society*, **4**, ISSN: 2392-473X (2017).

[5] Anderson. A theoretical study of the ionospheric F region equatorial anomaly-I. Theory. *Planetary and Space Science*. **21**: 409–419 (1973). doi: 10.1016/0032-0633(73)90040-8.

[6] Hanson, W. B. and Moffett, R.J. Ionization transport effects in the equatorial F region. *Journal of Geophysical Research*. **71**: 5559–5572 (1996). doi: 10.1029/JZ071i023p05559.

[7] Hajra, R.; Chakraborty, S. K. and Paul, A.. Electrodynamical control of the ambient ionization near the equatorial anomaly crest in the Indian zone during counter electrojet days, *Radio Sci*., **44**, RS3009 (2009).
doi:10.1029/2008RS003904.

[8] Liu, L.B.; Wan, W.X.; Ning, B.Q. And Zhang, M.L. Climatology of the mean total electron content derived from GPS global ionospheric maps. *Journal of Geophysical Research*. **114**: A06308 (2009). doi: 10.1029/2009JA014244.

[9] Chapagain, N.P. Dynamics of Equatorial Spread F Using Ground-Based Optical and Radar Measurements. All Graduate Theses and Dissertations, Utah State University, USA, https://digitalcommons.usu.edu/etd/897 (2011).

[10] Chapagain, N. P. Electrodynamics of the low-latitude thermosphere by comparison of zonal neutral winds and equatorial plasma bubble velocity, Journal of Institute of Science and Technology, ISSN: 2469-9062 (print), 2467-9240(e) 20(2): 84-89 (2015).

[11] Meng, Y.; An, J.C.; Wang Z.M., and E D.C. Spatial distribution of Antarctic ionosphere TEC based on GPS. Acta Geodaetica et CartographicaSinica. **40**: 37–40 (2011).

[12] Gupta, J.K. and Singh, L. Long term ionospheric electron content variation over Delhi, *Ann. Geophys (Germaney)*, **18**, pp 1635-1644 (2001).

[13] Chakraborty, S.K. and Hajra, R. Solar control of ambient ionization of the ionosphere near the crest of the equatorial anomaly in the Indian zones, *Bull Astron Soc India (India)*, 2007, **35**, pp 599-605 (2001).

[14] Bagiya, M. S.; Joshi, H. P.; Iyer, K. N. ; Aggrawal, M.; Ravindran, S. and Pathan, B.M. TEC variations during low solar activity period (2005-2007 near the equatorial ionospheric anomaly crest region in India, *Ann. Geophys. Germaney)*, **24**, pp 1047 -1057 (2009).

[15] Komjathy, A. Global Ionospheric Total Electron Content Mapping using the Global Positioning System. Ph.D. Thesis, University of New Brunswick, Canada, pp 1-265 (1997).

[16] Shim, J.S. Analysis of Total Electron Content (TEC) Variations in the Low- and Middle Latitude Ionosphere. Doctorial physics dissertation, Utah State University. http://digitalcommons.usu.edu/etd/403 (2009).

[17] Markovic, M. Determination of Total Electron Content in the Ionosphere Using GPS Technology, *Typology*, **627**. 7 (2014). DOI:10.14438/gn.2014.20.

[18] Chauhan,V.; Singh, O.P. and Singh, B. Diurnal and Seasonal variation of GPS-TEC during a low activity period as observed at a low latitude station Agra, *Indian Journal of Radio and Space Physics*, pp. 26-36 (2011).

[19] Dabas, R.S.; Bhuyan, P.K.; Tyagi, T.R. ; Bhardwaj, R.K. and Lal, J.B. Day to day changes in ionospheric electron content at low latitudes, *Radio Sci. (USA)*,**19**, pp 749-756 (1984).

[20] Chamberlain, J. W. Theory of Planetary Atmospheres, http://utd500.utdallas.edu/ionosphere.htm.

[21] Chapagain, N. P., B. G. Fejer, and J. L. Chau. Climatology of postsunset equatorial spread F over Jicamarca, J. Geophys. Res., 114, A07307 (2009). doi:10.1029/2008JA013911.

[22] Adhikari, B. HILDCAA-Related Effects Recorded in Middle Low Latitude Magnetometers, Doctorate Thesis of the Graduate Course in Space Geophysics, Instituto Nacional dePesquisas Espaciais, Sao Jose dos Campos, Brasil (2015). http://urlib.net/8JMKD3MGP3W34P/3J3GH78.

[23] Schunk, R.W. and Nagy, A. F. Ionospheres, Cambridge Univ. Press, New York (2000).

[24] Gonzalez, W. D.; Joselyn, J. A.; Y. Kamide, Y.; Kroehl, H. W.; Rostoker, G.; Tsurutani, B. T. And Vasyliunas, V. M. What is a geomagnetic storm qm?, *Journal of Geophysical Research*, vol. **99**, 5771–5792 (1994).

[25] Su, Y. Z.; Bailey, G. J. and Balan N. Modelling studies of the longitudinal variations in TEC at equatorial-anomaly latitudes, *J. Atmos. Sol. Terr. Phys.*, **57**11(4) , 433-442 (1995).

[26] Rodger, A.S.; Wrenn, G.L. and H. Rishbeth, H. Geomagnetic Storms in the Antartic F-region II Physical interpretation, *J. Atmos. Terr. Phys*., **51**, 851–866 (1989) (1989).

[27] Yamamotol, A.; Ohta, Y.; Okuzawa, T; Taguchi, S.; Tomizawa, I. and Shibata, T. Characteristics of TEC variations observed at Chofu for geomagnetic storms. *Earth Planets Space*, **52**, 1073–1076 (2000).

[28] Mendillo M. and Klobuchar, J. A. Investigations of the ionospheric F region using multistation total electron content observations, *J. Geophys.***80**, 643–650 (1975).

[29] Biqiang, Z.; Weixing, W.; Libo, L.; and Tian, M. Morphology in the total electron content under geomagnetic disturbed conditions: results from global ionosphere maps, *Ann. Geophys*., **25**, 1555–1568 (2007).

[30] Fuller-Rowell, T.J.; Codrescu, M.V.; Moffett R.J. and Quegan, S. Response of the thermosphere and ionosphere, J. *Geophys.* **99** (A3), 3893–3914 (1994). doi:./10.1029/93JA02015.

[31] Mendillo, M. Storms in the ionosphere: Patterns and processes for total electron content, *Rev. Geophys.*, 44 (2006) RG4001. (2006) doi:./10.1029/2005RG000193. /Wiley Online Library | 25bda6e0Web of Science® Times Cited: 88.

[32] Buonsanto, M. J. Ionospheric storms—A review, *Space Sci. Rev.*, **88**, 563–601 (1999).

[33] Chigomezyo, M. N.; Lee-Anne, M.; Pierre, J.C. And Anthea, J.C. Ionospheric observations during the geomagnetic storm events on 24–27 July 2004: Long-duration positive storm effects. *Journal of Geophysical Research*, **117** (2012). doi**:** 10.1029/2011JA016990.

[34] Niraj, B.; Chapagain, N.P.; and Adhikari, B. Total Electron Content and Electron Density Profile Observations during Geomagnetic Storms using COSMIC Satellite Data. *Discovery*, 1979-1996 (2016).